BACKGROUND OF CAPACITY INTERPRETATION USING DYNAMIC PILE MEASUREMENTS

By Garland E. Likins, Jr.

Measurements taken during impact pile driving have increased dramatically in the last two decades. In many sections of the world, electronic measurements on piling jobs are now the normal procedure rather than the exception. Their use now includes monitoring of pile stresses, hammer energy transfer efficiency, the calculation of pile capacity for determining criteria or quality control, and investigating the structural integrity of piles (1,2,3). While uses other than capacity determination are very important, they are rather straightforward computationally. This paper will therefore be addressed toward the field calculations and interpretations of capacity.

The dynamics of a pile during impact can be completely defined by three interconnected variables, namely, the forces and motions of the pile and the boundary conditions due to the soil. Knowledge of any two of these variables allows the computation of the third; measured pile top force and acceleration allow the closed form solution of soil resistance effects. Research begun at Case Western Reserve University in the early 1960's has led to a reuseable system for obtaining analog measurements of force and acceleration (2) which interrupt the driving operation by typically only five minutes per pile.

For interpreting these signals an insight into one-dimensional wave propagation is useful. The general equation of motion of a longitudinal wave in a bar is

$$\frac{\partial^2 u}{\partial t^2} = c^2 \frac{\partial^2 u}{\partial x^2}$$

with a general solution

$$u = f(x + ct) + f_1(x - ct)$$

implying two waves each travelling in the opposite direction and that superposition is valid. For a compression wave the particle velocity v is in the same direction as the velocity of wave propagation, but in a tension wave the velocity v is in the opposite direction. If two waves travelling in opposite directions come together the resultant force is obtained by addition and the resultant particle velocity by subtraction. Two such identical compressive waves travelling in opposite directions result therefore in a doubling of the stress and zero net velocity and hence zero displacement. This condition describes a fixed end. If the stress waves have opposite signs the stresses cancel and the velocities double, the free end condition. These closed form solutions for simple boundary conditions have been available since St. Venant. A series of examples are given to demonstrate the dynamics of pile driving and the reader is encouraged to find proof elsewhere (4) for important results.

In a uniform unsupported elastic pile, a stress wave will travel unchanged through the rod width at a speed which can be calculated from

$$c = \sqrt{E/\rho} \tag{1}$$

where E is the material modulus of elasticity and ρ is the mass density. The particle velocity of some point along the pile length can therefore be computed if it is known at some other point along the pile at a different time. A stress wave suddenly applied at the end of a rod causes the rod to be deformed. This deformation is transmitted along the rod. After time Δt the stress has travelled a distance $c\ \Delta t$, and the end of the rod

will have displaced an amount due to the strain ε

$$\delta = \varepsilon(c\,\Delta t) = \frac{\sigma}{E} c\,\Delta t$$

The velocity at the end of the rod is

$$v = \frac{\delta}{\Delta t} = \frac{\sigma}{E} c$$

Thus the input force ($F = \sigma A$) at the pile top is seen to be proportional to the input velocity by

$$F = \frac{EA}{c} v \tag{2}$$

as long as no upward travelling waves from resistance or rod end reflections are felt. As a convention throughout the rest of this paper v will be the particle velocity and V will be the velocity v times the pile impedance EA/c.

Let us examine the case of a pile with zero soil resistances. The input compressive wave is seen travelling down the pile in Figure 1a and 1b. When the wave arrives at the bottom (Figure 1c), the force wave reflects in tension, and to maintain the dynamic balance the pile end accelerates again (the velocity wave reflects with the same sign causing a doubling effect). The wave then travels up the pile (Figure 1d). The velocity wave still has a continually downward sign and the force is now a tension wave. In other words, the pile is now being pulled down due to the lack of soil resistance, and this pull is generating a tension force. When the force wave gets back to the pile top, it again reflects now in compression being a free end, causing a net force of zero at the pile top. The velocity again reflects with the same sign and travels back down the pile. The velocity at the pile top is again doubled.

Instead of looking at the stress and velocity distributions in the whole pile, we look at a particular point on the pile; the force and velocity waves

can easily be obtained. The pile top force velocity curves can be computed with time as shown in Figure 1e. Initially force and velocity waves are of the same magnitude. After the initial input, the force will always be zero due to the free ends and zero resistances. The particle velocity at the top at every 2L/c interval (the time necessary for the stress wave to travel from the pile top to the toe and return to the top) will become twice the input velocity magnitude. The force and velocity with time at the pile middle can also be computed, as shown in Figure 1f. There the input force and velocity wave arrive at a time L/2c after the initial impact at the top. Every time the wave passes the midpoint, the velocities are always the same. Every time the wave travels upward, the forces are in tension. When the wave reflects from the top and travels downward the forces are in compression.

For this case with zero pile resistances and free conditions at both the top and pile bottom, the force at a point can be computed if the velocity at that point is known by the equation

$$FPS(t) = V(t) - 2V(t - \frac{2L}{c}) + 2V(t - \frac{4L}{c}) - 2V(t - \frac{6L}{c}) \ldots. \quad (3)$$

where L is the length below the known velocity location to the pile bottom. This equation is quickly verified by inspection of Figures 1e and 1f. Equation 3 is then known as the free pile solution; that is, the force required at a location with known velocities at that location having zero resistances on the pile.

A second analysis can be done assuming a fixed top and a fixed bottom. In this analysis the assumption is that there is resistance at the pile ends. The wave travelling down in Figure 2a arrives at the bottom in Figure 2b,

causing a compressive reflection of force and no pile end movement at the bottom (the velocity reflects with the opposite sign cancelling the input velocity wave). This condition will be satisfied if the resistance at the pile bottom shows a rigid plastic behavior with a resistance at least equal to twice the input force; otherwise the pile will move, violating the fixed condition. Figure 2c shows the wave as it travels up the pile after the first reflection. The force is again in compression, but the velocity is negative; the pile rebounds. At the fixed pile top, the force again reflects in compression and superimposes on the upwards travelling initial reflection wave, and the velocity reflects with a changed sign causing zero net displacement at the pile top (Figure 2d). The pile top and pile mid-section force and velocity waves are shown in Figures 2e and 2f. In this case, the force at 2L/c at the pile top, and every 2L/c thereafter, is twice the input force magnitude and the velocity is zero at the pile top, due to the fixed condition. At the pile middle, each passage of the wave generates a compression force. The velocity is positive if the wave is travelling downward and negative if travelling upward.

Figure 3 shows the results of a resistance force located at the pile mid-point. For demonstration, we assign a rigid plastic resistance force of one-half of the input force magnitude. The arrival of the input stress wave at the pile mid-point will produce resistance waves which travel upward in compression and downward in tension, each with half the magnitude of the resistance force, or in this example, one quarter of the force input. The effect on velocity will be to generate waves of negative sign travelling in both the upward and downward directions. The net force travelling down the

pile (Figure 3b) is reduced due to the superposition of the input wave and the generated negative resistance wave, and an upward travelling wave is generated in compression. When the wave gets to the bottom (Figure 3c), assuming again a free bottom free top condition, the downward input force reflects in tension. The downward tension resistance force reflects in compression. At the same time the upward travelling compression wave reflects in tension. The velocities reflect with the same sign, the positive input reflects positively and the resistance velocity waves reflect negatively, and Figure 3d shows the wave's arrival at the pile top. Figure 4a shows the pile top forces and velocities with time for this assumed resistance case. Note that until a time L/c the force and velocity waves are unaffected and the solution is similar to the free pile. After that time the force and velocity waves separate, by a magnitude equal to the resistance which was applied at the pile mid-point. At time 2L/c the velocities seem to increase to the original downward input magnitude. After the initial input, the force is always zero. The result of a free pile solution (Equation 3) for Figure 4a is also shown in Figure 4. The difference between this free pile solution from Equation 3 and the observed force is a measure of the resistance acting on the pile. The difference, called the measured delta curve, is the measured force minus the free pile solution. The measured delta curve for Figure 4a is shown in Figure 4b. As observed, the measured delta curve, at time L/c rises to a magnitude equal to the applied resistance at the pile mid-point, and at time 2L/c rises to the magnitude of twice the resistance. Figure 5a shows an assumed measured force and velocity curve. By obtaining a free pile solution (Figure 5b) and then a measured delta curve (Figure 5c), the total capacity of the pile can be obtained as half the value of the measured delta curve at time 2L/c.

As the delta curve at time 2L/c is equal to

$$\Delta(2L/c) = F(2L/c) - FPS(2L/c)$$

where

$$FPS(2L/c) = V(2L/c) - 2V(0)$$

thus since V equals F at impact (time 0)

$$\Delta(2L/c) = F(2L/c) - (V(2L/c) - V(0) - F(0)).$$

As seen in Figure 5c, the delta curve at time 2L/c is equal to twice the resistance. Substitution of 2RT for $\Delta(2L/c)$ yields

$$RT = (F1 + F2 + V1 - V2)/2 \qquad (4)$$

where 1 indicates the impact time and 2 the time 2L/c later. Equation 4 is the Case Method capacity equation (2). A quick computation with equation 4 on the free pile example shows zero resistance ((4 + 0 + 4 - 8)/2 for the top and (4 - 4 + 4 - 4)/2 for the middle) as it should. Computation for the fixed end case shows a resistance of twice the input force ((4 + 8 + 4 - 0)/2 equals 8 versus input 4). Although the resistance may be more this is all that can be mobilized. Calculation for the case with side resistance gives half the input force ((4 + 0 + 4 - 4)/2 equals 2 versus input 4) which is the value we originally assigned to this resistance.

Equation 4 has often erroneously been associated with the assumption that the soil resistances require a rigid plastic model. Such is not the case. Square wave pulses as used here provide the easiest to understand presentations. However, the same conclusions could be made with triangle or any other general curve. In relation to the soil resistance assumed in Figure 3, an elastic plastic soil law could have been used with a general input pulse.

As long as the displacement reached at each point along the pile before the arrival of the peak velocity at that point exceeds the quake (displacement where the soil model goes plastic), Equation 4 will be valid.

The delta curve concept can be used to determine where resistances are located. The value of the measured delta curve at time t before 2L/c is equal to the sum of the soil resistances above the location x(= ct/2) on the pile (see Figure 5c). The soil resistance between two points on a pile is then the difference between the measured delta curve for those points.

An example demonstrating this technique is shown in Figure 6. The pile was a 12 inch (300mm) closed end pipe pile with a cross sectional area of 9.8 square inches (63.2cm^2) driven into silty clay. The data is from a restrike after a static load test. Shown with the measured force and velocity curves in Figure 6a are the free pile solution and measured delta curve which has a maximum value of 363 kips (1617kN) implying a total resistance of 181 kips (808kN).

In actuality the resistance in Equation 4 can be either static or damping. Figure 6b shows the results of applying either shear or damping resistances at the pile bottom. In the case of shear, the resistance delta curve rises and retains the static load. For the damper, the load increases to a maximum as the wave arrives at the damper and then decreases as the velocity of the pile decreases. Thus the total resistance can perhaps be separated into static and damping components by investigating what happens to the delta curve after 2L/c.

The delta curve peak at 2L/c in Figure 6a is then probably due to velocity or damping effects. The residual value may be due to static forces.

Using the damping approach as derived elsewhere (2) with

$$RS = RT - J(F1 + V1 - RT) \tag{5}$$

a value for the Case Method damping constant J can be determined from the delta curve interpretations of RS and RT. Rearranging gives

$$J_{\Delta} = (RT - RS) / (F1 \,\&\, V1 - RT). \tag{6}$$

Comparison of J_{Δ} with empirical J values determined from the soil borings, can be used as a check on Case Method damping constants, thus providing an extra degree of confidence if no further technique is available (i.e. Equation 6 can also be used with static load test results or CAPWAP total capacity, or previous piling experience with similar local soil conditions).

For the presented example, the static resistance is estimated at 75 kips (334kN) based on half the residual value of the delta curve after 2L/c. Solution of Equation 6 yield a value of 1.12 for J_{Δ} which is high for the assumed silty clay soil where an empirical J of 0.55 had been suggested for this soil type. Use of this empirical J led to a capacity of 129 kips (575kN) whereas the static test failed at 81 kips (361kN). This data set had been the worst case of all static-dynamic correlations obtained to date (2). The static resistance determined from the delta curve is in much better agreement (93%) than the value obtained from the observed soil type (159%). It is possible that the soil type was not classified correctly or that the silt particles were very fine, almost clay particles in size.

A comparison of the skin friction as obtained directly from the measured delta curve and from strain gages along the pile length is shown in Figure 6c. The delta curve presented a direct measure of the RT distribution.

By ratioing RT with RS, the forces in the pile at ultimate load are obtained and are seen to be in excellent agreement with the loads obtained by static testing.

Although the preceding solution technique has definite usage in skin friction distribution, it is not so simple to determine RS. Several factors combine to limit the usefulness of this technique. First the skin friction has a reducing effect on the delta curve after 2L/c as seen in the example presented in Figure 4. The delta curve could be modified to convert skin to equivalent toe resistance by

$$\Delta_m(t) = \Delta(t) + \Delta(t - 2L/c) \tag{7}$$

for times t less than 4 L/c after the initial wave onset at the top. However, this modified delta now contains all damping resistances and the time of pile toe zero velocity (where damping is also zero) must be determined. The time where

$$4V(t - \frac{2L}{c}) = \Delta_m(t) \tag{8}$$

has been suggested (1). However the correlation of RS determined by this technique is not as good as that obtained by other methods (2).

An additional problem is that in hard driving, the bottom velocity becomes negative causing unloading very early. The shear delta curve then begins to look similar to that for the damper as the resistance begins unloading (Figure 6b) so that distinguishing between the two becomes difficult.

In easy driving, Equation 8 may never be satisfied and damping therefore non zero. The derived RS, even if the minimum delta is chosen, may therefore be too large.

Therefore, the exact interpretation of the delta curve after 2L/c is difficult at best. A more rigorous analysis such as CAPWAP is much better

suited to sorting out static resistances from damping. A minimum RS can be found from the delta curve or maybe even a maximum value from the modified delta curve. Engineering judgements may often be required.

Once RS has been determined, the reduced delta curve defined by

$$\Delta_r(t) = 2\Delta(t) \; RS/\Delta(2L/c) \tag{9}$$

can be used as shown in Figure 6c to produce very realistic resistance distributions.

SUMMARY

The closed form solution to the equation of motion of a wave in an elastic rod has been presented. Several theoretical boundary conditions have been described in detail. The Case Method capacity equation has been informally derived, and ways to separate static and damping resistances have been shown. The skin friction distribution can be estimated from the measured delta curve.

REFERENCES

1. Goble, G.G., Rausche, F. and Moses, F., "Dynamic Studies on the Bearing Capacity of Piles, Phase III," Report No. 48, Division of Solid Mechanics, Structures and Mechanical Design, Case Western Reserve University, 1970.

2. Goble, G.G., Likins, G.E. and Rausche, F., "Bearing Capacity of Piles from Dynamic Measurements", "Final Report", March 1975, Case Western Reserve University, Cleveland, Ohio.

3. Goble, G.G., Rausche, F. and Likins, G.E., "The Analysis of Pile Driving-A State-of-the-Art," Seminar on the Application of Stress-Wave Theory on Piles, Stockholm, Sweden, June 1980.

4. Timoshenko, S. and Goodier, J.M., Theory of Elasticity, McGraw-Hill, Second Edition, 1951, p. 438.

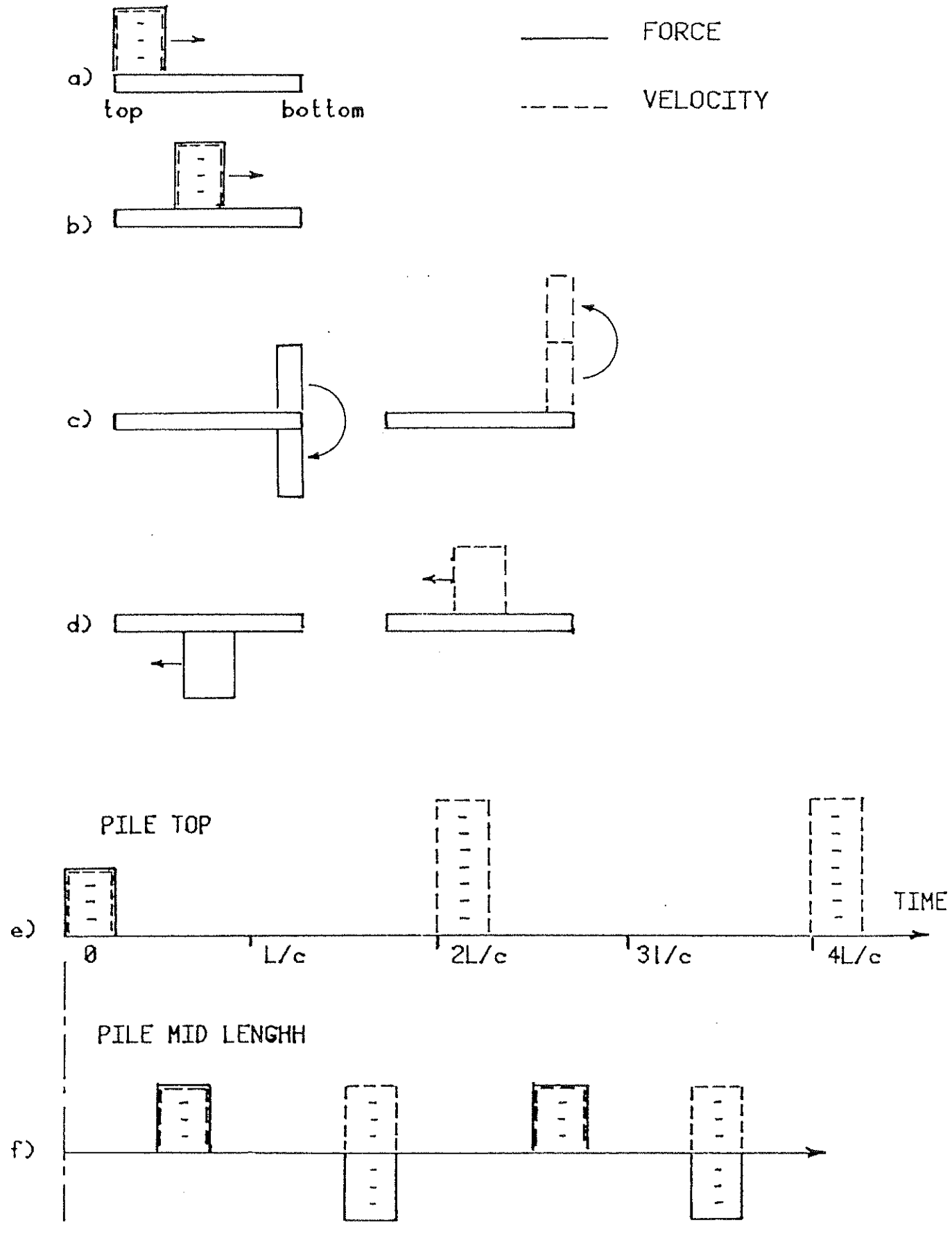

FIGURE 1 PILE WITH ZERO RESITANCE. FREE TOP AND BOTTOM

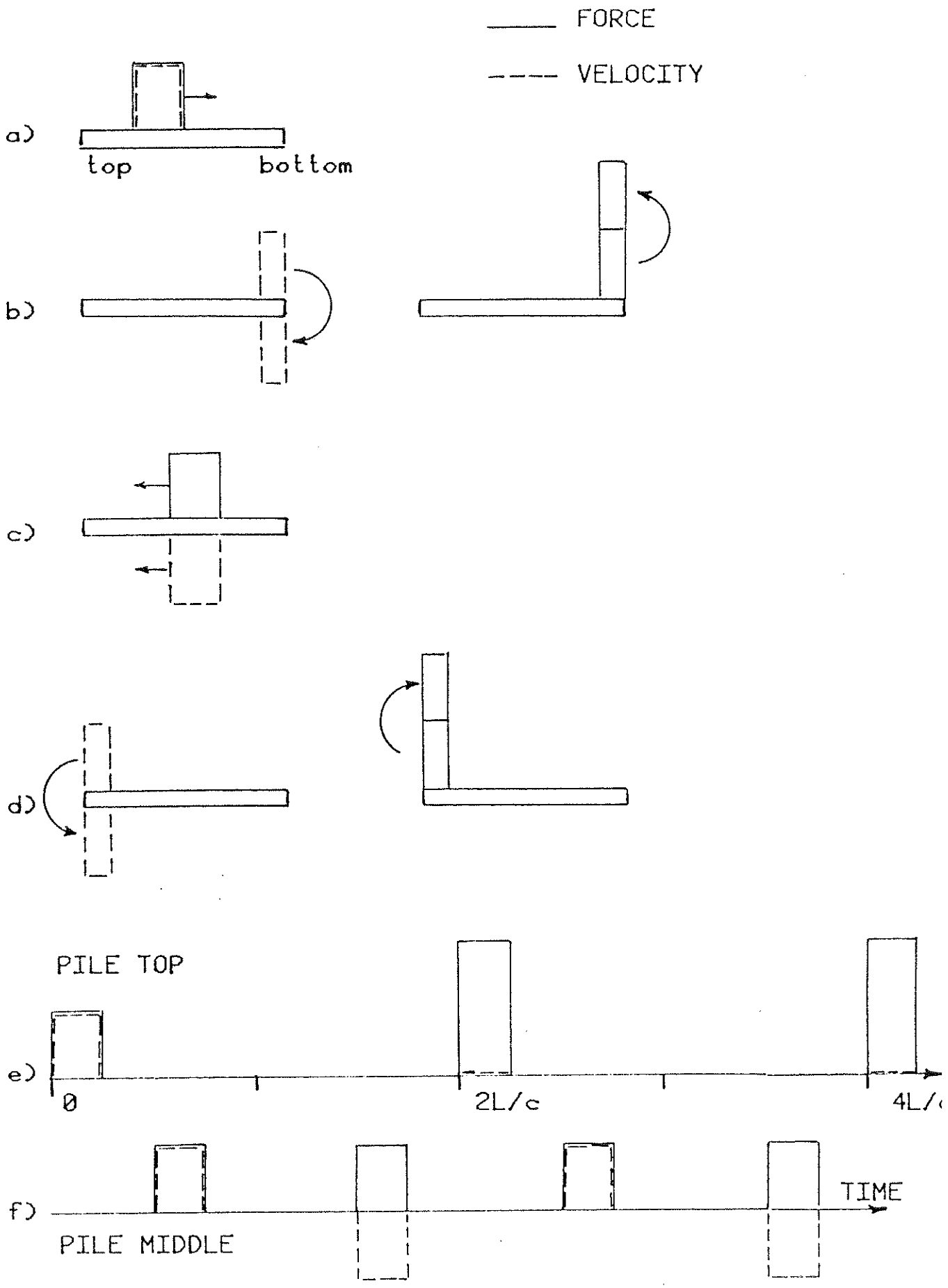

FIGURE 2 PILE WITH FIXED TOP AND BOTTOM

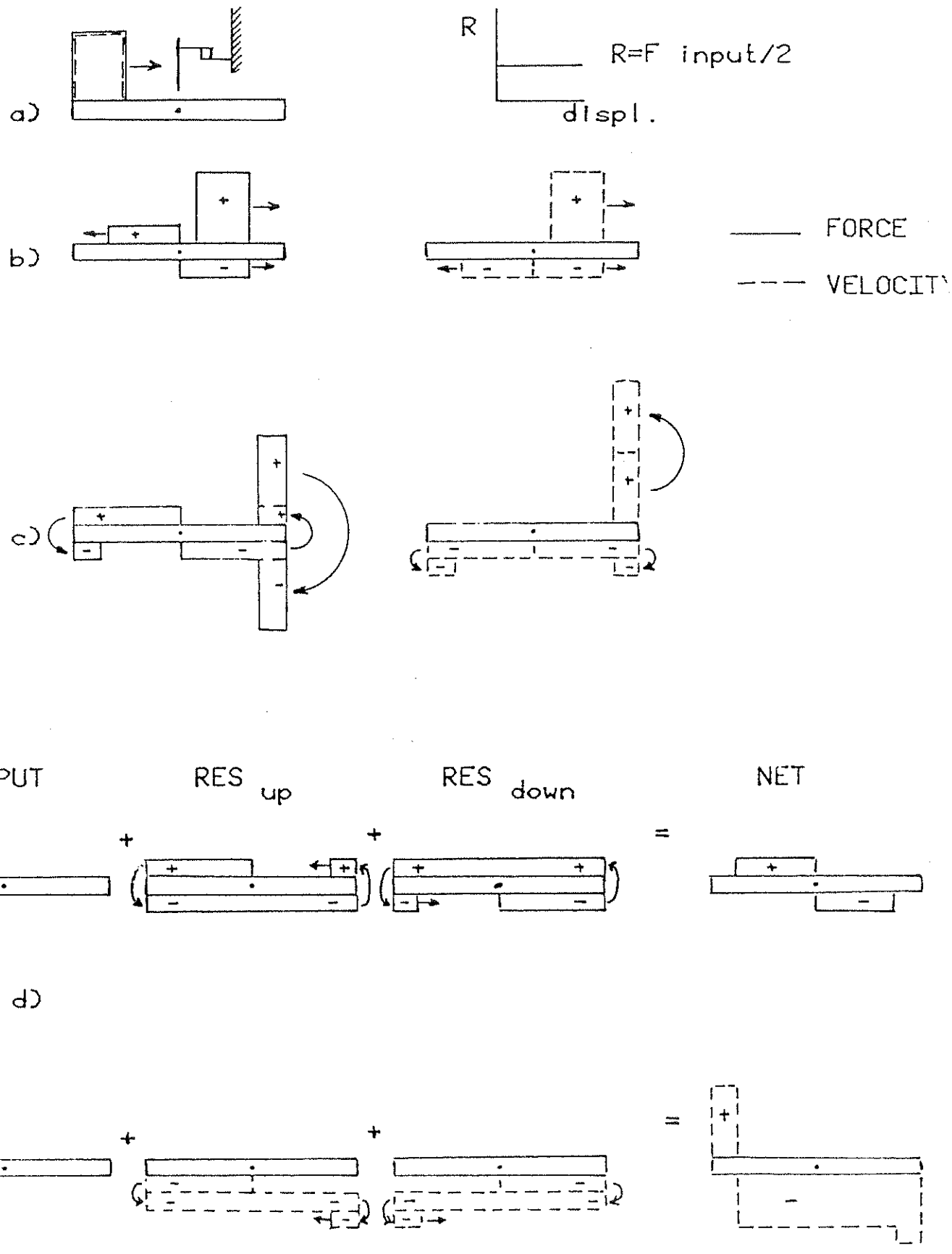

FIGURE 3 PILE WITH FREE TOP AND BOTTOM, RESISTANCE AT MIDPOINT WITH MAGNITUDE EQUAL TO HALF INPUT FORCE PEAK

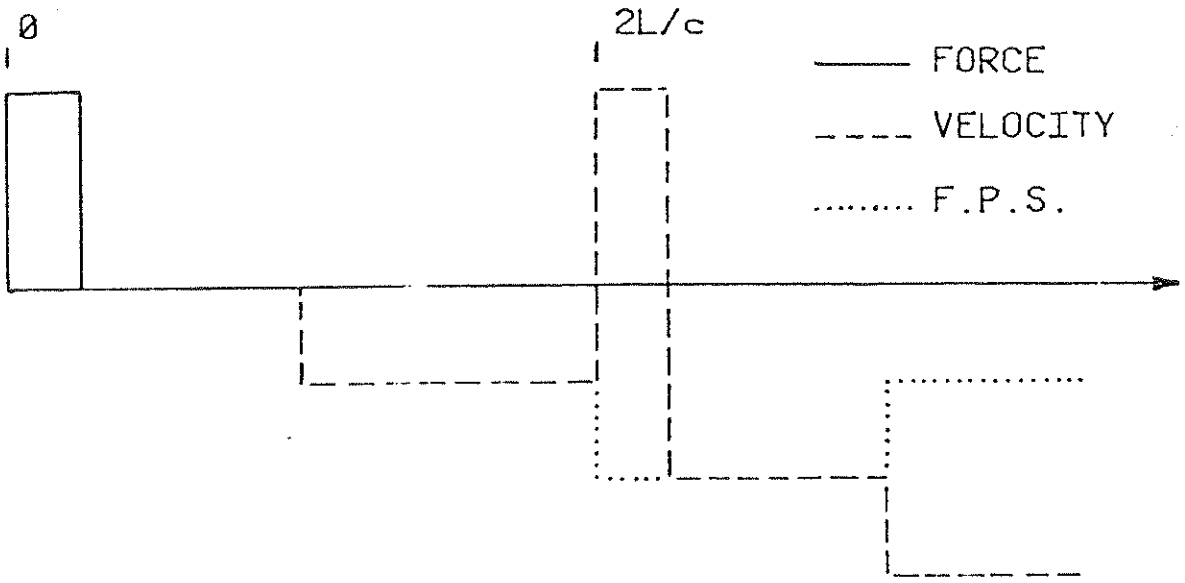

a) PILE TOP EFFECT FOR FIGURE 3

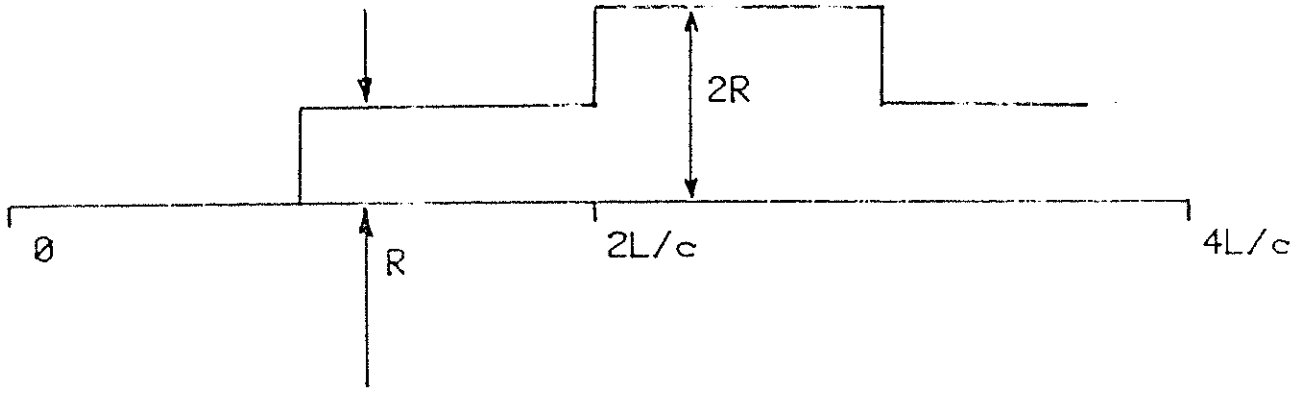

b) MEASURED DELTA CURVE FOR FIGURE 3

FIGURE 4

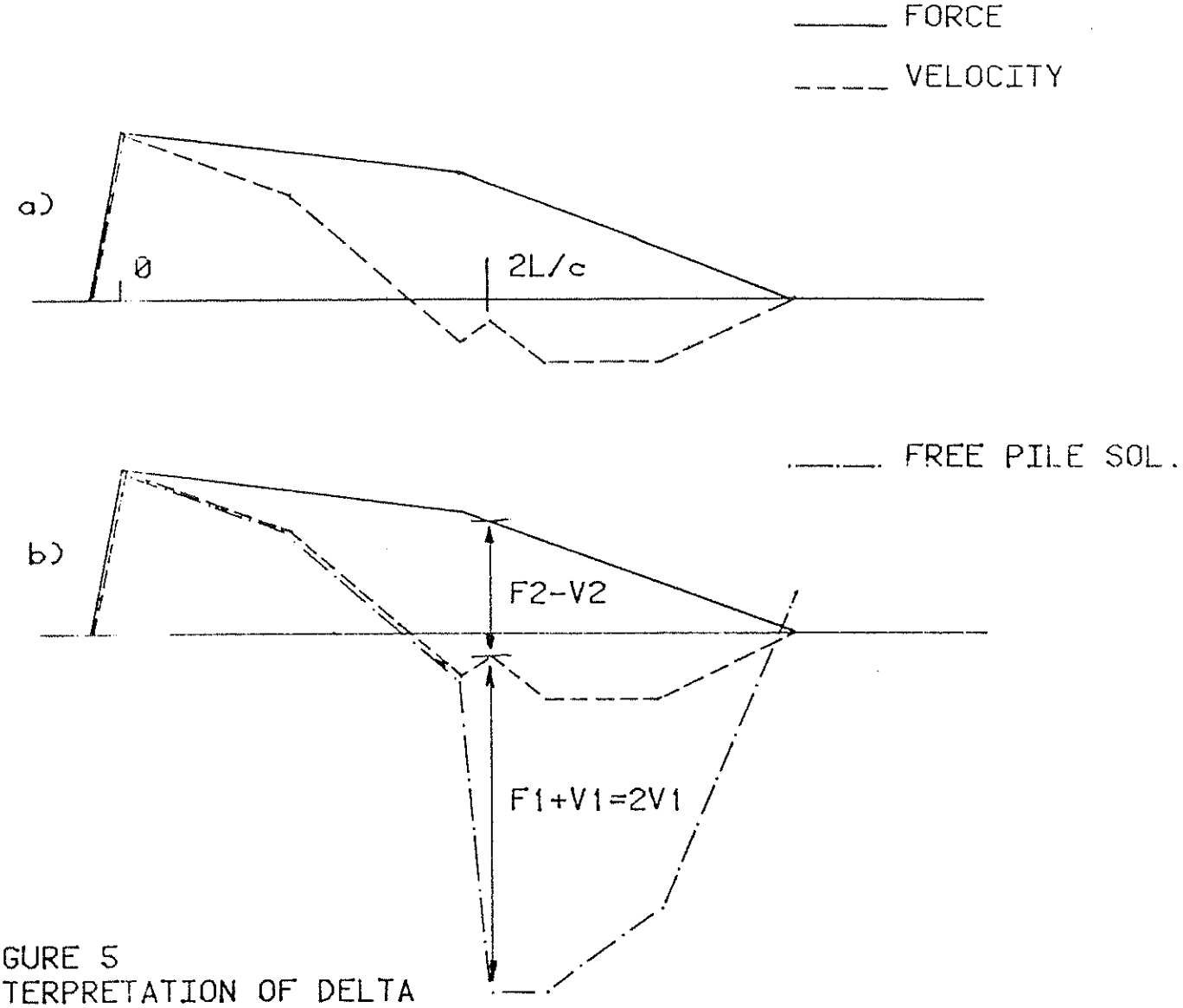

FIGURE 5
INTERPRETATION OF DELTA

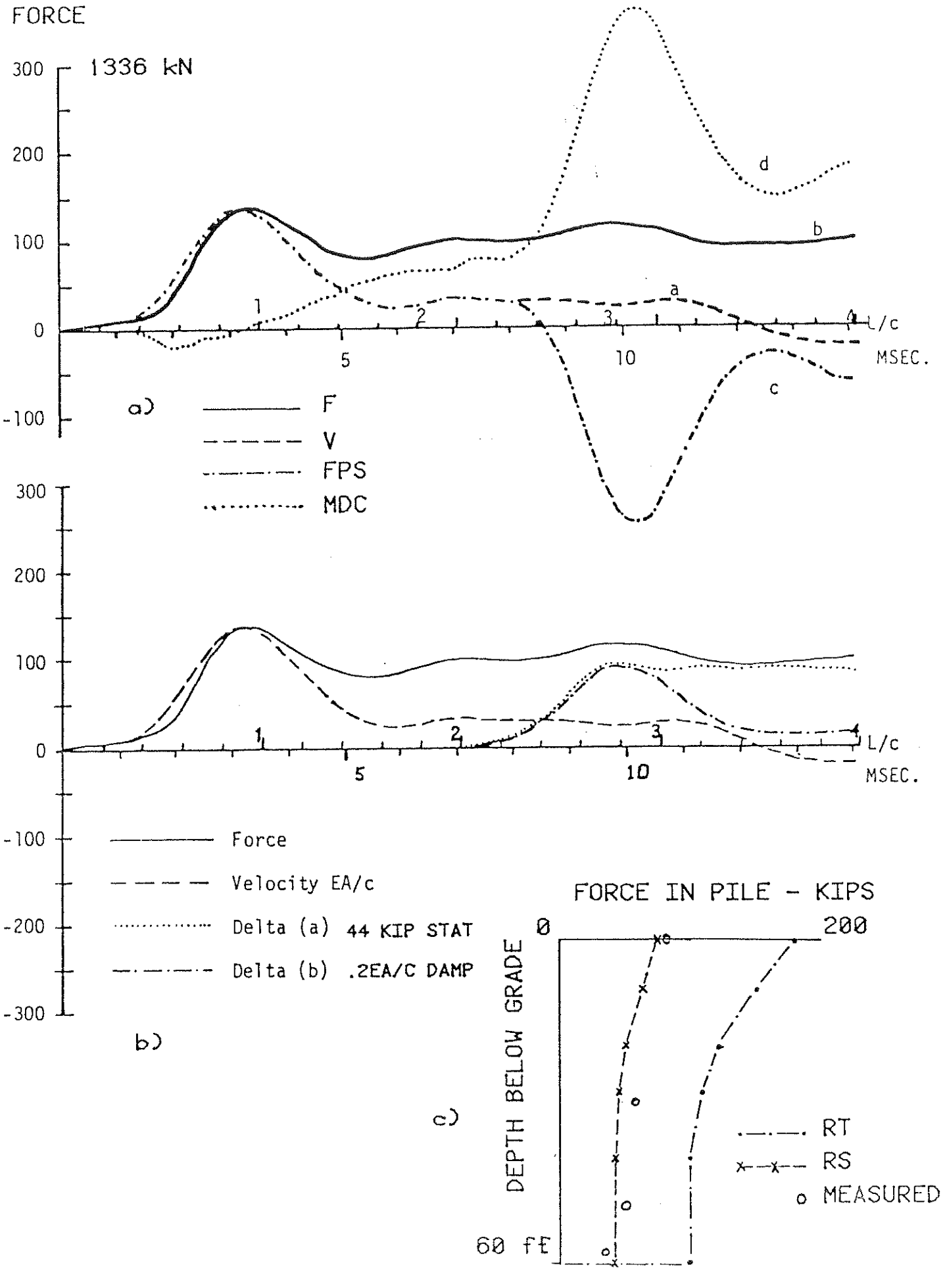
FORCE
1336 kN
300
200
100
0
-100
a)
F
V
FPS
MDC
d
b
a
c
1
2
3
4
L/c
5
10
MSEC.
300
200
100
0
-100
-200
-300
Force
Velocity EA/c
Delta (a) 44 KIP STAT
Delta (b) .2EA/C DAMP
b)
FORCE IN PILE - KIPS
0
200
DEPTH BELOW GRADE
60 ft
c)
RT
RS
MEASURED

1981
BOULDER SEMINAR

Background of Capacity Interpretation
Using Dynamic Pile Measurements
By Garland E. Likins, Jr.

High Tension Stresses in Concrete Piles
During Hard Driving
By Garland E. Likins, Jr.

Load & Resistance Factor
Design of Piles
By G. G. Goble

Case Method
By Garland E. Likins, Jr.
and Frank Rausche